LIMNOLOGY and OCEANOGRAPHY

ASLO

Limnol. Oceanogr. 71, 2026, e70293

doi: 10.1002/lno.70293

RESEARCH ARTICLE

Methane emission intensifies the warming effect of carbon dioxide efflux from a subtropical coastal macroalgae aquaculture ecosystem

Yueting Deng,[1,2,3,4] Xianghui Guo [1,3,5], Dengjin Hu,[6] Hui Luo,[3,4] Yougan Chen,[5,7] Xudong Zhu [1,2,3,4,7*]

[1]State Key Laboratory of Marine Environmental Science, Xiamen University, Xiamen, Fujian Province, China; [2]Key Laboratory of the Coastal and Wetland Ecosystems (Ministry of Education), Xiamen University, Xiamen, Fujian Province, China; [3]National Observation and Research Station for the Taiwan Strait Marine Ecosystem (Xiamen University), Zhangzhou, Fujian Province, China; [4]College of the Environment and Ecology, Xiamen University, Xiamen, Fujian Province, China; [5]College of Ocean and Earth Sciences, Xiamen University, Xiamen, Fujian Province, China; [6]Fujian Provincial Key Laboratory of Coast and Island Management Technology, Fujian Institute of Oceanography, Xiamen, Fujian Province, China; [7]Shenzhen Research Institute of Xiamen University, Shenzhen, Guangdong Province, China

Abstract

Macroalgae aquaculture ecosystems have been increasingly recognized as coastal biogeochemical hotspots of air–sea net ecosystem carbon dioxide (CO_2) exchange; however, their roles in regulating the temporal variability of net ecosystem methane (CH_4) exchange (NME) receive little attention mainly due to very limited data availability. Here, we applied the eddy covariance (EC) technique to acquire 1-yr (June 2023 to May 2024) NME measurements, over a subtropical macroalgae aquaculture ecosystem in southeast China, to examine the temporal variability of NME across time scales and its contribution to net radiative forcing. The results indicated that (a) this ecosystem acted as a CH_4 source in most months with the summer accounting for about two-thirds of annual NME of 0.40 g C m^{-2} yr^{-1}; (b) the inclusion of annual NME increased the sustained-flux global warming potentials (SGWPs) by 11.0% from 219.3 (CO_2 only) to 243.4 g CO_2-eq. m^{-2} yr^{-1} for a 100-yr time horizon; (c) NME and its radiative contribution varied across seasons, farming periods, and growth stages, with the temporal fluctuations mainly controlled by temperature and tidal activities; (d) bimodal varying patterns across tidal levels were identified with larger fluxes occurring when tidal level changed most rapidly. This is the first EC study to confirm that CH_4 emission intensifies the warming effect of CO_2 efflux from macroalgae aquaculture ecosystems. The observed strong temporal variability of CH_4 and CO_2 fluxes and their asynchrony highlight the importance of high-frequency and continuous flux measurements in accurately assessing their net radiative forcing at both short- and long-term scales.

Macroalgae ecosystems have attracted more and more attentions in climate change mitigation because of their high primary production and carbon sequestration capacity compared to other coastal ecosystems (Krause-Jensen and Duarte 2016; Ortega et al. 2019; Queirós et al. 2019; Duarte et al. 2022). In addition to restoring natural macroalgae habitats, macroalgae aquaculture with sufficient cultivation area has recently garnered a lot of attention as a natural way to reduce greenhouse gases (GHGs) in the atmosphere (Bach et al. 2021; Gao et al. 2022). Macroalgae aquaculture is a massive global industry, with China occupying the largest cultivation area of 1252–1265 km^2 (Wu et al. 2020). Global macroalgae ecosystems have been found to sequester 173 Tg C of atmospheric carbon dioxide (CO_2) annually (Krause-Jensen and Duarte 2016); however, methane (CH_4) emission from these ecosystems has been often neglected (Al-Haj and Fulweiler 2020). Research has indicated that the coastal marine environment is a significant atmospheric CH_4 source and actually contributes 0.21 Pg CO_2-eq. yr^{-1} to global CH_4 emission (Rosentreter, Borges, et al. 2021; Resplandy et al. 2024). The availability of in situ CH_4 flux measurements in coastal macroalgae ecosystems is very limited, which results in large uncertainties in the estimation of CH_4 emission that hinders our efforts to promote the application

*Correspondence: xdzhu@xmu.edu.cn

Associate editor: Ruth Reef

of macroalgae aquaculture in terms of its role in climate change mitigation.

Coastal vegetated habitats provide sediment conditions that are favorable to high CH_4 production because of the surplus organic matter resulting from extremely high primary production and the accumulation of allochthonous particulate organic matter (Ortega et al. 2019; Roth et al. 2022; Hall et al. 2025). Previous studies have shown that CH_4 production in coastal waters primarily arises from methanogenesis in anoxic sediments (Ferrón et al. 2010; Hou et al. 2016). The CH_4 consumption, occurring through anaerobic oxidation within sediments and aerobic oxidation within water columns (Knittel and Boetius 2009; Al-Haj and Fulweiler 2020), reduces the produced CH_4 and thus net emission into the atmosphere at the air–sea interface. Diffusion, ebullition and plant-mediated transport are the three main pathways by which CH_4 is released from sediments to the atmosphere in shallow coastal vegetated ecosystems (Jeffrey et al. 2019; Hilt et al. 2022). The former two emission pathways (i.e., diffusion and ebullition) are easily influenced by changing pressure conditions regulated by hydrodynamic factors such as tides and winds, leading to highly transient and pulsed CH_4 flux on short timescales (Roth et al. 2022). Hence, pulse CH_4 emission may occur from time to time given the high heterogeneity and variability of coastal environments. Overall, CH_4 production, consumption, and transport involve complex processes that are modulated by a variety of direct and indirect factors, resulting in large temporal heterogeneity of CH_4 flux (Rosentreter, Al-Haj, et al. 2021).

The CH_4 flux and its contribution to the radiative forcing in macroalgae ecosystems may be inaccurately assessed due to a lack of enough in situ observations. On the one hand, coastal CH_4 flux studies with high-frequency measurements focus on traditional blue carbon ecosystems including mangrove (J. Liu et al. 2020), saltmarsh (X. Zhu et al. 2025), and seagrass (Yau et al. 2023), while there are few such studies n macroalgae habitats, especially for macroalgae aquaculture. On the other hand, the exploration of the magnitude and temporal dynamics of CH_4 flux may be impacted by the limitations of observing methods. Prior studies on CH_4 flux in coastal vegetated ecosystems have mostly used the chamber-based methods, which normally cover daytime-only measurements at the risk of missing large CH_4 emissions at night (Podgrajsek et al. 2014; Y. P. Zhang, Qin, et al. 2022; X. Zhu, Chen, et al. 2024). Meanwhile, the CH_4 budget is typically assessed using short-term field measurements on a few consecutive days, which is prone to bias the aggregation when summed up to monthly or even longer time scales (Hou et al. 2016; Y. P. Zhang, Qin, et al. 2022; Roth et al. 2023). In addition, CH_4 emission via the pulse ebullition might not be covered by the short-term chamber measurements, which could lead to an obvious underestimation of CH_4 emission (Al-Haj and Fulweiler 2020). Furthermore, different anthropogenic managements across aquaculture stages can also significantly affect the magnitude and temporal variability of CH_4 flux (Y. P. Zhang, Qin, et al. 2022; Xiong et al. 2024). With the rapid turnover of macroalgae biomass and sediment accumulation rates (Attard et al. 2019; Hurd et al. 2022), the macroalgae aquaculture areas may behave as biogeochemical hotspots of air–sea CH_4 exchange (Lundevall-Zara et al. 2021; Hall et al. 2025).

The CH_4 flux derived from the high-frequency and continuous eddy covariance (EC) measurements represents the net CH_4 flux as a result of the processes of CH_4 production, consumption, and transport, compensating for the limitations of traditional chamber-based methods. As an automatic and non-destructive in situ flux measuring technique, the EC approach can quantify multiple GHG fluxes simultaneously (e.g., CH_4 and CO_2) (X. Zhu et al. 2019; Baldocchi 2020). Although the EC approach has been widely used in various ecosystems, including coastal wetlands (J. Liu et al. 2020; Y. Zhang et al. 2023; X. Zhu, Chen, et al. 2024), it has rarely been applied to coastal macroalgae aquaculture ecosystems that are highly productive and globally distributed. In this study, we used the EC approach to measure net ecosystem exchange of CH_4 and CO_2 for one full year over the sea–air interface in a semi-enclosed macroalgae aquaculture bay in southeast China. The key aims of this study are (1) to examine the temporal variability of CH_4 fluxes across diurnal, daily, and seasonal scales and their environmental controls, and (2) to assess the importance of CH_4 fluxes in affecting the radiative forcing induced by CO_2 fluxes in coastal macroalgae aquaculture ecosystems. This study will provide an important piece of direct evidence on high-frequency air–sea CH_4 fluxes in macroalgae aquaculture ecosystems, which helps to improve the understanding of their GHG flux dynamics and radiative forcing across time scales.

Materials and methods

Study area and aquaculture management

The GHG flux tower (26.7218°N, 119.9871°E; ChinaFLUX) in the study area is located in the Sansha Bay macroalgae aquaculture area in Fujian Province, China (Fig. 1), which has a subtropical monsoon climate with irregular semi-diurnal tides (mean tidal range of 5.35 m). Sansha Bay is a semi-enclosed bay with its baymouth just 3 km wide connecting to the East China Sea. *Saccharina japonica* and *Gracilariopsis lemaneiformis* are the two primary farming types in this macroalgae aquaculture area, with the former cultivated from December to May of the next year and the latter be cultivated all year round. There is also a portion of the fish raft around the flux tower for *Apostichopus japonicus* (sea cucumber) cultivation, with the cultivation cycle from roughly November to March of the next year.

Greenhouse gas fluxes and ancillary measurements

The GHG fluxes (i.e., CH_4 and CO_2) in this study referred to air–sea net ecosystem exchange of CH_4 (NME) and CO_2 (NEE) between the aquaculture ecosystem and the atmosphere, where

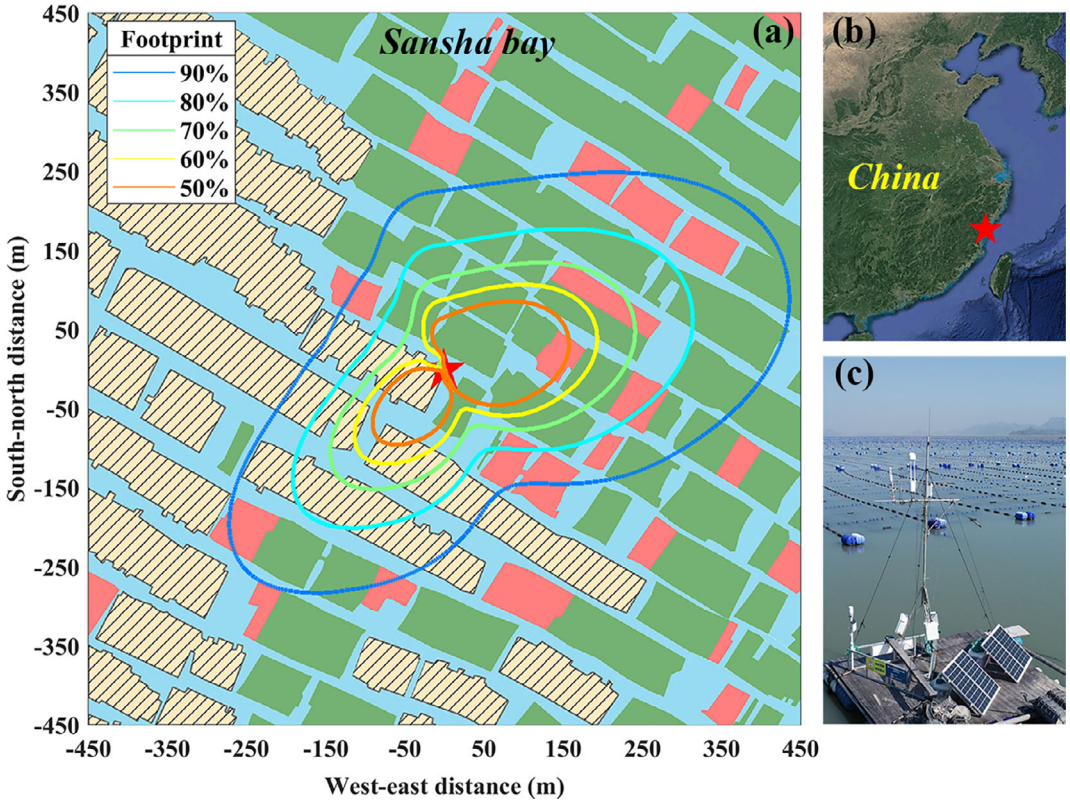

Fig. 1. The eddy covariance flux tower (red star) was deployed over the macroalgae aquaculture area (mapped from a drone image acquired on January 26, 2024) overlaid by the flux footprint climatology (**a**) in a subtropical enclosed bay in southeast China (Sansha Bay) (**b**). The tower was fixed to a large fish raft to reduce potential swaying issues (**c**). Green, red, yellow, and blue blocks indicate *Saccharina japonica*, *Gracilariopsis lemaneiformis*, *Apostichopus japonicus* cultivations, and seawater, respectively. Note that there was a slight spatial relocation (< 500 m apart) of the tower in mid-July 2023 due to the unintended removal of the original fish raft attached with the tower.

NME denoted the net flux of CH_4 production and consumption and NEE represented the balance between CO_2 influx (e.g., via gross primary production) and CO_2 efflux (e.g., via ecosystem respiration). The meteorological sign convention was employed to indicate the GHG fluxes, where positive and negative values denoted upward (emission) and downward (uptake) fluxes, respectively. The NME and NEE were derived from the measurements by an EC system, consisting of two open-path gas analyzers of CH_4 (Li-7700, Li-COR Inc.) and CO_2 (Li-7500, Li-COR Inc.) and a three-axis sonic anemometer (CSAT-3, Campbell Scientific, Inc.) (Fig. 1c). The EC system was installed $\sim$ 5 m above the water surface of the macroalgae aquaculture area, with 90% of the fluxes contributing from the aquaculture area within $\sim$ 400 m around the tower based on the footprint climatology analyses following Kormann and Meixner (2001) (Fig. 1a). The gas analyzers' sensor mirrors were routinely cleaned approximately once a week to ensure the quality of the measurements.

An integrated weather station (ATMOS 41, METER Group, Inc.) was used to collect the meteorological data including solar radiation, wind speed, air temperature, and rainfall in this study. Water quality parameters from a nearby buoy device included water temperature, dissolved oxygen, and salinity, measured by a CTD sensor (SBE 37 SMP-ODO, Sea-bird). Tidal level data were derived from the tidal forecast table of a nearby site within Sansha Bay (Zhangwan site from State Oceanic Administration of China). Drone and satellite imagery were combined to map the evolution of primary aquaculture types over the studying period (Fig. 1a). A high-performance Attitude and Heading Reference System Ellipse-A (SBG system) attitude system was utilized to continuously record the attitude data for 1 month (December 2023), which were used for flux corrections due to the swaying issue of the platform following Edson et al. (1998). Given that we had only 2-month attitude data and the correction only caused a 3% relative deviation, further data analyses were based on the fluxes without the attitude correction to ensure consistency.

Flux processing and statistical analyses

The raw 10-Hz EC data over the 1-yr studying period, from June 2023 to May 2024, were processed into 30-min time-series data using the EddyPro software (Li-COR Inc.) with a series of flux corrections (including axis rotation, frequency response correction, ultrasonic correction, and Webb-Pearman-Leuning correction) and quality control (including steady-state test, turbulent conditions test, statistical test, and absolute limits test) processes (X. Zhu, Hou, et al. 2021;

X. Zhu, Qin, et al. 2021; Y. Zhang et al. 2023; X. Wang and Zhu 2024). The 30-min data were assigned with quality flags using the 0–1–2 system (Mauder et al. 2013) (i.e., the flag of 0, 1, and 2 stands for the best-, good-, and poor-quality data, respectively), and the data with a flag of 2 were excluded in this study. The 30-min flux data under conditions of rainfall and insufficient nighttime turbulence were also discarded. Specifically, a friction velocity threshold was calculated for each 3-month time window over the year and then applied to exclude nighttime fluxes below the friction velocity threshold (Papale et al. 2006). To prevent low-quality data from possible contamination of Li-7700 mirrors, NME data with a relative signal strength indicator of less than 20% were also eliminated. Due to the unbalanced data availability between daytime and nighttime, we, respectively, performed quality control for daytime and nighttime data to mitigate the bias in the aggregation to daily and monthly data (Y. Liu and Zhu 2024). The days with valid 30-min records less than 25% of the total number of records were not incorporated into the daily and monthly scales (X. Zhu, Sun, et al. 2021; Z. Zhu and Zhu 2025). Annual NME and NEE were estimated by summarizing their respective monthly values. Over the 1-yr study period, after excluding poor data due to quality issues and instrument failures, the percentages of valid 30-min NME and NEE data were 65.7% and 66.2%, respectively. The percentages of valid daily NME and NEE accounted for 83.1% and 92.9%, respectively. To match the EC data, all ancillary measurements were converted into 30-min time series data for further analyses.

To better analyze NME across various farming periods and stages, we separated the 1-yr studying period into the following periods based on the dominant farming activities (Table 1): from December 2023 to May 2024 for *S. japonica* farming period (December and January for the rapid growth stage, February and March for the middle growth stage, and April and May for the harvesting stage); June, July, October, and November 2023 for *G. lemaneiformis* farming period. August and September 2023 were considered as non-farming (seawater) periods without macroalgae cultivation. Mean diurnal variation analyses were used to examine diurnal variation in NME. To examine the environmental controls on NME, principal component analysis and Spearman's correlation analysis were applied to 30-min time series data of NME and environmental factors. To compare the radiative forcing of NME (RF_{CH_4}) and NEE (RF_{CO_2}) and their net combination (RF_{net}), we converted them into CO_2 equivalent (CO_2-eq.) using the SGWP metric (Neubauer and Megonigal 2015), where the conversion value of 45 was used for CH_4 for a 100-yr time horizon (Eq. 1).

$$RF_{net} = RF_{CH_4} \times 45 + RF_{CO_2} \quad (1)$$

Positive and negative radiative forcing values represented warming and cooling effects, respectively, from NME, NEE, or their net combination. To explore the tidal impacts, we followed our previous study (Deng et al. 2025) to divide the 30-min data even into six groups by tidal level (i.e., 1H–6H denoted six equal parts from low to high tidal levels) and treated 1H and 6H (3H and 4H) as the "slow" ("fast") tidal current group. All data processing and statistical analyses were performed in MATLAB R2024b software (MathWorks, Inc.).

Results

Temporal variations in environmental factors

The 1-yr measurements showed that daily and monthly environmental factors in the study area exhibited strong seasonal variations (Fig. 2). Daily cumulative solar radiation ranged from 3.1 to 76.6 MJ m^{-2} d^{-1}, with maximum solar radiation occurring in July. Throughout the year, daily wind speed had strong fluctuation with an average value of 3.1 m s^{-1}. Rainfall was concentrated in August and September, with the maximum daily rainfall of 134 mm over the year. Daily air temperature ranged between 4.2°C and 33.2°C, while daily water temperature ranged between 12.8°C and 30.3°C. Water quality factors also showed large seasonal fluctuations, with mean dissolved oxygen and salinity of 6.4 mg L^{-1} (4.1–8.4 mg L^{-1}) and 29.8 ppt (28.3–32.4 ppt), respectively. Daily maximum tidal level ranged from 6.1 to 8.8 m with peaking monthly spring tide in October.

Temporal variations in GHG fluxes

Large fluctuations in GHG fluxes were also observed on daily and monthly scales (Fig. 3). Daily NEE ranged from −2.3 to 1.5 g C m^{-2} d^{-1} with the mean value of 0.2 g C m^{-2} d^{-1}, and monthly NEE varied from the largest source of 18.7 g C m^{-2} $month^{-1}$ in August to the largest sink of −13.5 g C m^{-2} $month^{-1}$ in December. Over the year, this ecosystem acted as a CO_2 source of 59.8 g C m^{-2} yr^{-1}. Daily CH_4 flux ranged from −7.3 to 9.2 mg C m^{-2} d^{-1} (mean value of 1.1 mg C m^{-2} d^{-1}). For most of the study period, the macroalgae aquaculture area acted as a net source of CH_4 with the largest emission of 142.1 mg C m^{-2} $month^{-1}$ in July. Overall,

Table 1. Different periods with the dominant farming activities from June 2023 to May 2024.

2023						2024					
Jun	Jul	Aug	Sep	Oct	Nov	Dec	Jan	Feb	Mar	Apr	May
Gracilariopsis lemaneiformis		Non-farming		*Gracilariopsis Lemaneiformis*		*Saccharina japonica*					
						Rapid growth		Middle growth		Harvesting	

Note: "Non-farming" and Dec 2023 ~ May 2024 for "*Saccharina japonica*".

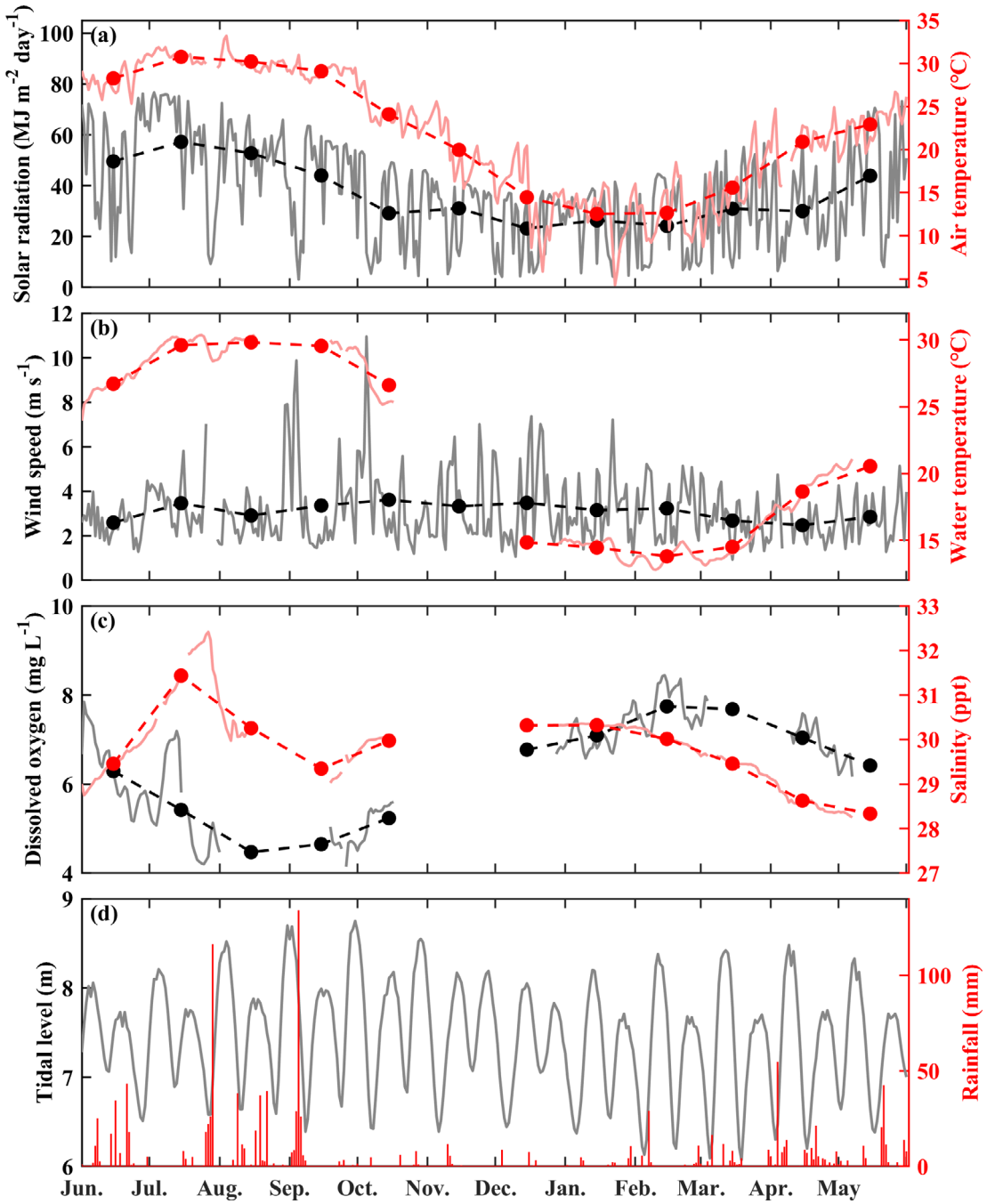

Fig. 2. Temporal variations in daily (lines/bar) and monthly (solid dots) environmental factors from June 2023 to May 2024, including (**a**) cumulative solar radiation, mean air temperature, (**b**) mean wind speed and mean water temperature, (**c**) mean dissolved oxygen, mean salinity, (**d**) maximum tidal level and cumulative rainfall.

summer had the strongest CH_4 emission with an average daily flux of 2.69 mg C m^{-2} d^{-1}, whereas autumn had the lowest CH_4 emission at 0.0057 mg C m^{-2} d^{-1} (*see* Supporting Information Fig. S1 for the comparisons of daytime, nighttime, and all-day NME among seasons). The mean diurnal variation analyses also confirmed the CH_4 emission source-sink pattern in this macroalgae aquaculture area (Fig. 4). The magnitude of the fluctuation in mean diurnal fluxes varied across seasons with the largest fluctuation occuring in spring from −1.99 to 3.16 mmol m^{-2} s^{-1}. All of the highest NMEs averaged over the daytime (2.45 mmol m^{-2} s^{-1}), nightime (2.79 mmol m^{-2} s^{-1}), and all-day (2.59 mmol m^{-2} s^{-1}) periods occurred in summer. There was no statistically significant difference in NME between daytime and nighttime periods (*see* Supporting Information

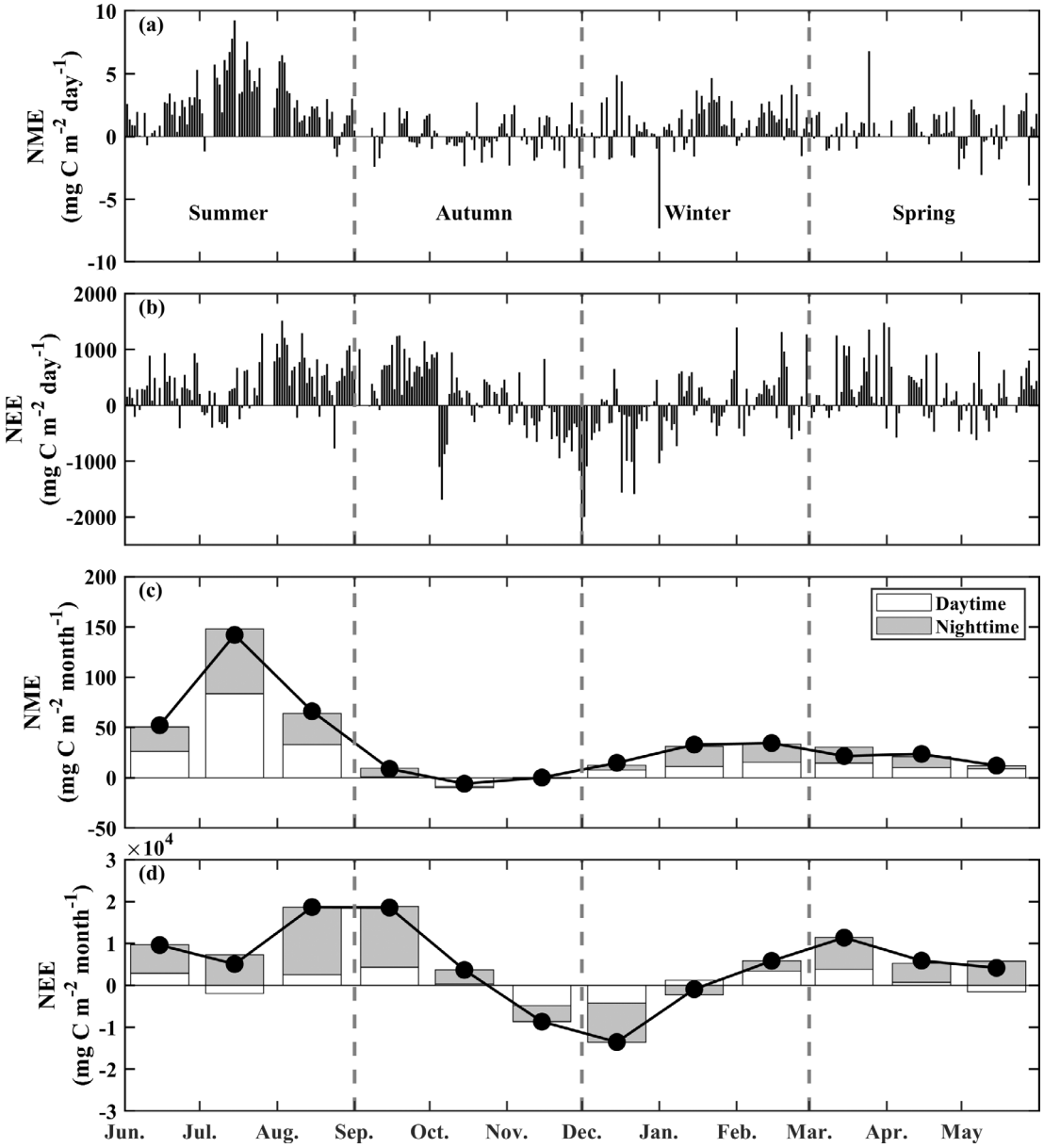

Fig. 3. Temporal variations in (**a**, **b**) daily and (**c**, **d**) monthly net ecosystem exchanges of CH_4 (NME) and CO_2 (NEE) over the macroalgae aquaculture from June 2023 to May 2024. NEE, net ecosystem exchange; NME, net ecosystem methane exchange.

Fig. S2 for monthly comparsions of daytime and nighttime NME).

Environmental controls on CH_4 fluxes

To better examine the relationships between NME and environmental factors, principal component analysis was used to explore the correlation between 30-min NME and environmental factors across different seasons and farming periods (Fig. 5). The analysis indicated that the initial two principal components explained 55.9% of the variance within the dataset. Specially, the primary component accounted for 36.3% of the variance with significant contribution from air temperature (54.3%), water temperature (56.6%), and dissolved oxygen (−52.2%). Observations aligned with the first principal component showed pronounced separation across winter, spring, and summer/autumn, indicating the influence of temperature on seasonal CH_4 flux dynamics. NME also showed a significant segregation between the kelp aquaculture period and other stages. The second principal component captured 19.6% of the variance, primarily driven by water level (64.7%). Spearman's rank correlation analysis was also applied to examine the relationships between 30-min NME and air temperature, water temperature, dissolved oxygen and water level across seasons (Fig. 6). The analysis indicated that the

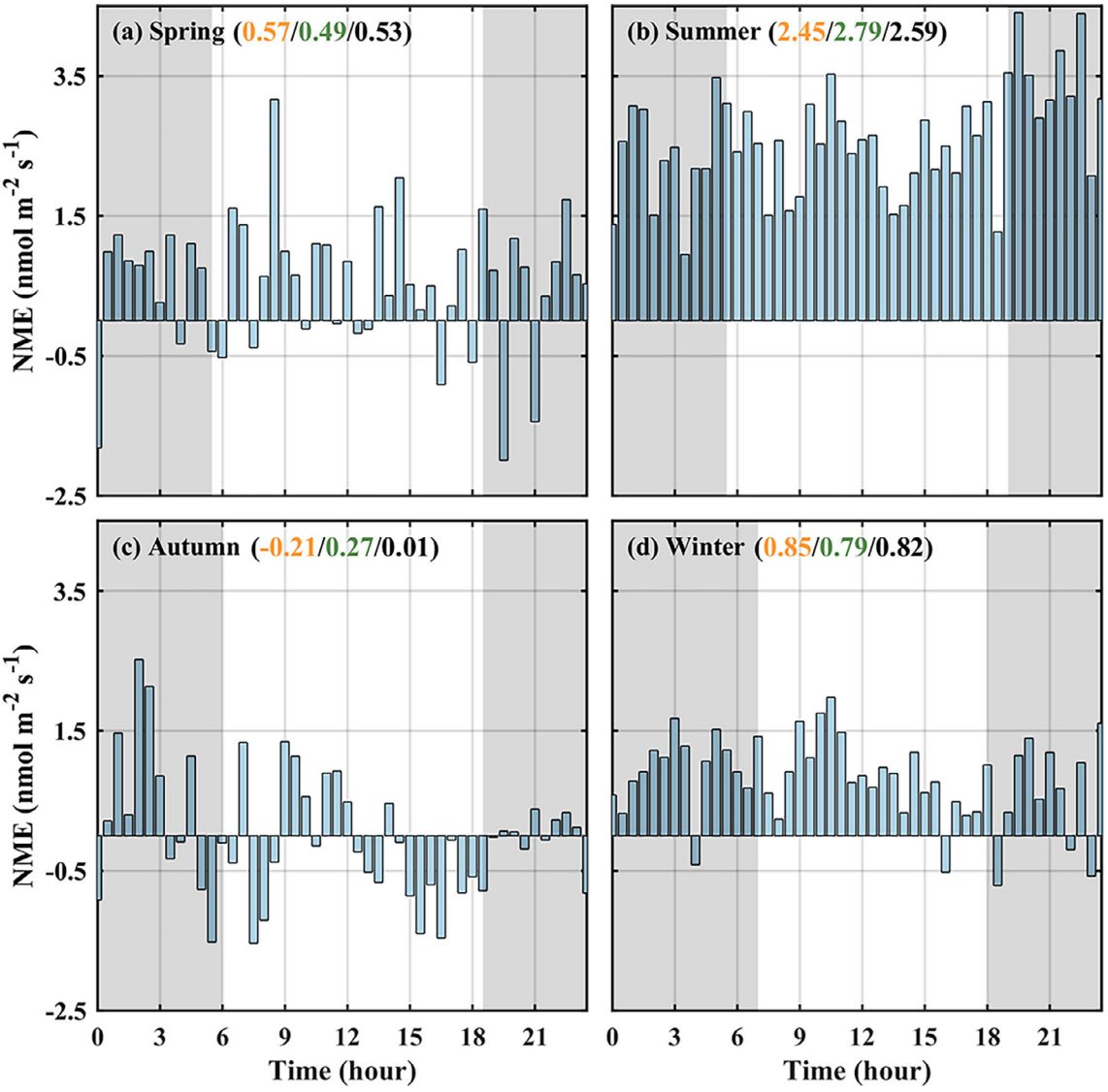

Fig. 4. Mean diurnal variations in net ecosystem exchange of CH_4 (NME) over the macroalgae aquaculture for each season. Daytime and nighttime are indicated by white and gray areas, respectively. The three values shown in the bracket for each season indicate the mean fluxes during the daytime, nighttime, and throughout the day based on the mean diurnal variation. NME, net ecosystem methane exchange.

best explanatory factor of NME changed across seasons. Net ecosystem methane exchange was best correlated with air/water temperature during spring and summer (statistically significant positive correlations at $p < 0.05$), while during autumn and winter, water level served as the best explanatory factor (statistically significant positive correlations). Dissolved oxygen exhibited a statistically significant negative correlation with NME only in summer. To further explore the links of GHG fluxes and tidal activities, the data were grouped according to different tidal levels (Fig. 7). The RF_{CH_4}, RF_{CO_2}, and their combination of RF_{net} tended to show bimodal varying patterns during both daytime and nighttime, having stronger radiative forcing values at faster tidal currents (when tidal level changed most rapidly; i.e., around 3H–5H) (*see* Supporting Information Fig. S3 for statistical comparisons among all tidal levels). The percentage of RF_{CH_4} over RF_{CO_2} ranged from 1.7% to 25.4% (excluding an extreme value with tiny NEE) across tidal levels with overall higher daytime values.

Temporal variations in global warming potentials

The relative strength of NME and NEE expressed as SGWP varied across seasons and farming stages for this macroalgae aquaculture area (Fig. 8). The CH_4 emission increased the warming effect caused by CO_2 emission throughout all seasons except winter. The largest and smallest enhancements occurred in summer (12.2%) and autumn (0.8%), respectively, while the CH_4 emission counteracted 44.2% of the cooling

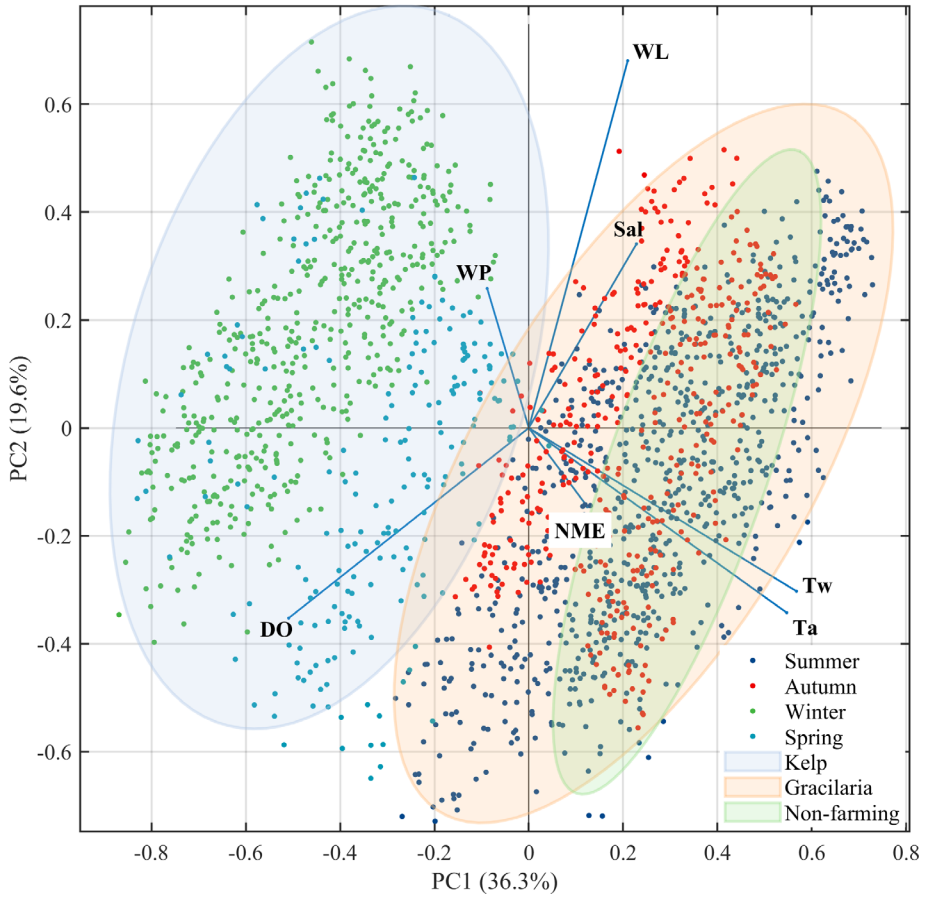

Fig. 5. Principal component analysis of the relationships between net ecosystem exchange of CH_4 (NME) and environmental factors, including air temperature (T_a), water temperature (T_w), water level (WL), dissolved oxygen (DO), and wind speed (WP). This biplot showed the distribution and the loadings of all factors along the first two principal components (PC1 and PC2). Each vector represents a factor with the direction and magnitude reflecting the contribution of the factor to each principal component axis. Close (symmetrical) vectors indicate a positive (negative) correlation, while orthogonal vectors indicate no correlation between the factors. NME, net ecosystem methane exchange.

effect due to CO_2 uptake in winter. In terms of farming periods, NME intensified the NEE-induced warming effect with comparable enhancements between kelp and *Gracilaria* farming periods and smaller enhancement for the non-farming period. During the rapid growth stage of kelp farming, NME offset 9.8% of the NEE-induced cooling effect, while NME enhanced the NEE-induced warming effect with comparable percentages between the middle growth and harvesting stages. On an annual basis, the CH_4 emission intensified the NEE-induced warming effect with a 11.0% increase, promoting the net radiative forcing from 219.3 to 243.4 g CO_2-eq m^{-2} yr^{-1}.

Discussion

CH_4 emission and its temporal variations

One-year high-frequency and continuous flux observations show that the macroalgae aquaculture area acts as a CH_4 source in most months with an annual emission of 0.40 g C yr^{-1}, which confirms the role of macroalgae aquaculture areas as potential CH_4 emission hotspots. This annual emission is comparable to CH_4 emission from natural macroalgae habitats in the Baltic Sea (0.25 g C yr^{-1}; Roth et al. 2023) and a macroalgae aquaculture area in Sanggou Bay (0.21 g C yr^{-1}; Hou et al. 2016), but lower than CH_4 emission from the coastal mariculture ponds (1.44 g C yr^{-1}; Y. F. Zhang, Tang, et al. 2022). In comparison with traditional blue carbon ecosystems, this annual emission is lower than the median annual emission in mangrove (1.22 g C yr^{-1}) and saltmarsh (0.98 g C yr^{-1}) but slightly higher than that in seagrass (0.28 g C yr^{-1}) (Al-Haj and Fulweiler 2020). Similar to many other coastal ecosystems (McNicol et al. 2017; Roth et al. 2023; Henriksson et al. 2024), large seasonal fluctuations occur in CH_4 fluxes in the study area. The peaking CH_4 emission in summer is presumably linked to enhanced methanogenesis at higher temperatures over the year (Yvon-Durocher et al. 2014). In addition to temperature, the CH_4 emission could also be

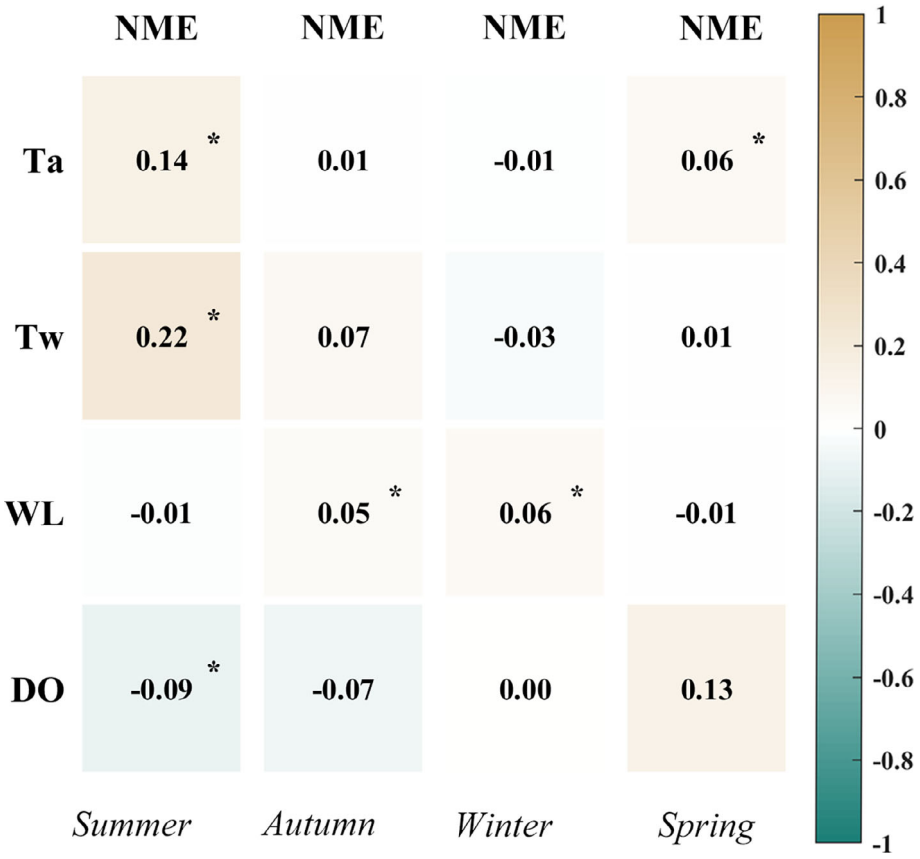

Fig. 6. Heatmaps of Spearman's rank correlations between 30-min net ecosystem exchange of CH_4 (NME) and environmental factors, including air temperature (Ta), water temperature (T_w), water level (WL), and dissolved oxygen (DO) across different seasons. The correlation coefficients were calculated on a pairwise basis, and the values with a star sign indicated statistical significance at $p < 0.05$. NME, net ecosystem methane exchange.

obviously affected by the substrate availability (Wallenius et al. 2021). For example, the second strongest CH_4 emission in this macroalgae aquaculture area is observed in winter instead of autumn that has the second highest temperatures (Figs. 2, 3). This may be due to the fact that the kelp farming in winter provides more substrate inputs for methanogenesis (Y. Wang et al. 2023; Pessarrodona et al. 2024), which in turn accelerates the production and release of CH_4 despite the lower temperatures (Dale et al. 2019). In terms of sub-daily variation, CH_4 flux exhibits no consistent diel variation with only marginal differences observed between daytime and nighttime emission. This small day–night difference could be explained by counteractive processes. On the one hand, daytime emission can be either promoted by stronger methanogenesis with higher temperatures and elevated labile substrates derived from photosynthesis (Bridgham et al. 2013). On the other hand, CH_4 emission can also be suppressed by stronger methanotrophy with more oxygen availability (or oxygen priming) from photosynthesis (Noyce et al. 2023). These counteractive effects are partially reflected by the correlation analysis showing that CH_4 emission is positively correlated with temperature in summer and spring but negatively correlated with dissolved oxygen in summer (Fig. 6).

Tidal controls in regulating CH_4 fluxes

Coastal vegetated habitats are experiencing fast environmental changes and thus the GHG flux dynamics are susceptible to a variety of factors such as the physical forcing drivers (e.g., tides), especially in the open coastal environment (Al-Haj and Fulweiler 2020; Roth et al. 2022; Arias-Ortiz et al. 2024; X. Zhu, Chen, et al. 2024). Bimodal flux variation patterns with tidal levels are observed in this study area, i.e., larger fluxes correspond to faster tidal currents when tidal level changes most rapidly (e.g., 3H–5H) (Fig. 7). This can be explained by the fact that faster tidal currents facilitate water column mixing and air–sea gas exchange. On the one hand, stronger water column mixing with sediment resuspension triggered by faster tidal currents may substantially enhance CH_4 production and bubble ebullition (Jordan et al. 2020), because microorganism concentrations in the sediments can exceed those in the water column by several orders of magnitude (Schmale et al. 2015). On the other hand, faster tidal currents with well-mixing turbulent conditions in surface water

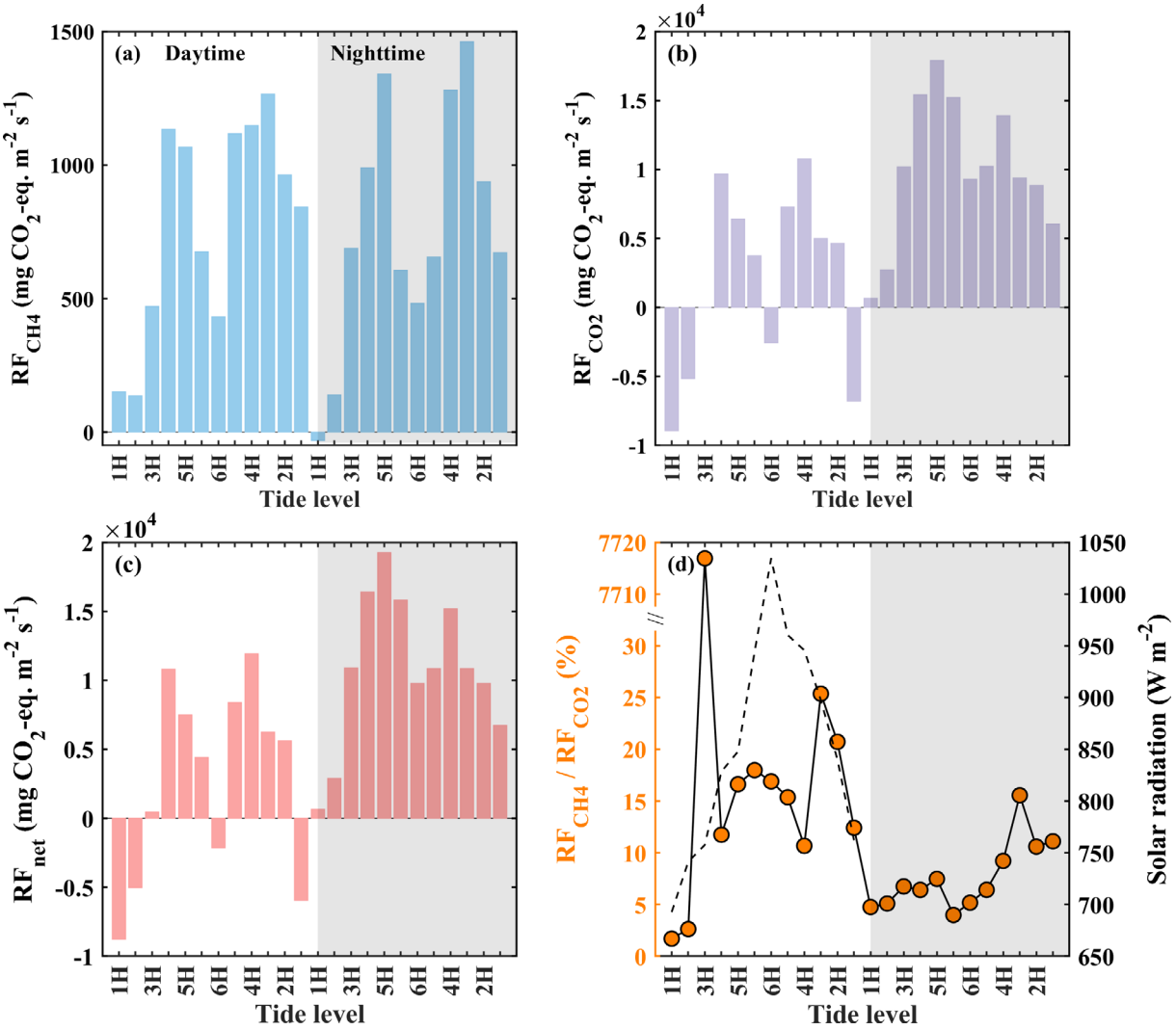

Fig. 7. Mean tidal variations in radiative forcing, using the sustained global warming potential metric, of (**a**) net CH_4 flux (RF_{CH_4}), (**b**) net CO_2 flux (RF_{CO_2}), (**c**) the net combination of RF_{CH_4} and RF_{CO_2} (RF_{net}), as well as (**d**) the percentage of RF_{CH_4} over RF_{CO_2} (overlaid by solar radiation) across tidal levels from low to high tide (1H–6H) for both daytime and nighttime periods. The tidal rule of 12ths was used to divide tidal levels into 12 groups from 1H (lower levels) to 6H (higher levels) and from 6H to 1H within a flood-ebb tidal cycle.

can substantially promote gas transfer velocity and thus speed up CH_4 emission into the atmosphere, since gas transfer velocity is a key control of gas exchange across the air–sea interface (Wanninkhof et al. 2009). Given that peaking solar radiation at noon roughly matches the highest tidal levels at daytime (Fig. 7d), the low value of the bimodal pattern at noon could also be associated with stronger methanotrophy with more oxygen supply from midday photosynthesis.

Asynchronous variations between GHG fluxes

The CH_4 emission exacerbates the positive radiative forcing from CO_2 efflux in this macroalgae aquaculture area, in contrast to the blue carbon offset effect reported by many other studies (Rosentreter et al. 2018; Roth et al. 2023; Yau et al. 2023; Li et al. 2024; X. Zhu, Chen, et al. 2024). The net radiative forcing varies considerably across different seasons and farming phases, with the strongest percentage contribution of CH_4 over CO_2 in winter rather than in summer with peaking CH_4 emission. This is mainly due to the asynchronous variations between CH_4 and CO_2 fluxes that are also reported in other coastal ecosystems (Roth et al. 2023; X. Zhu, Chen, et al. 2024). In this study, this asynchrony might mainly result from various farming activities, for example, kelp farming in winter not only promotes photosynthetic carbon uptake leading to a weaker CO_2 source but also provides more substrates for methanogenesis. Furthermore, when farming activities are not conducted, CO_2 emission increases dramatically, leading to a much smaller enhancement in the warming effect from CH_4 emission. The fluctuations in the percentage contribution of CH_4 over CO_2 can vary by one or two orders of

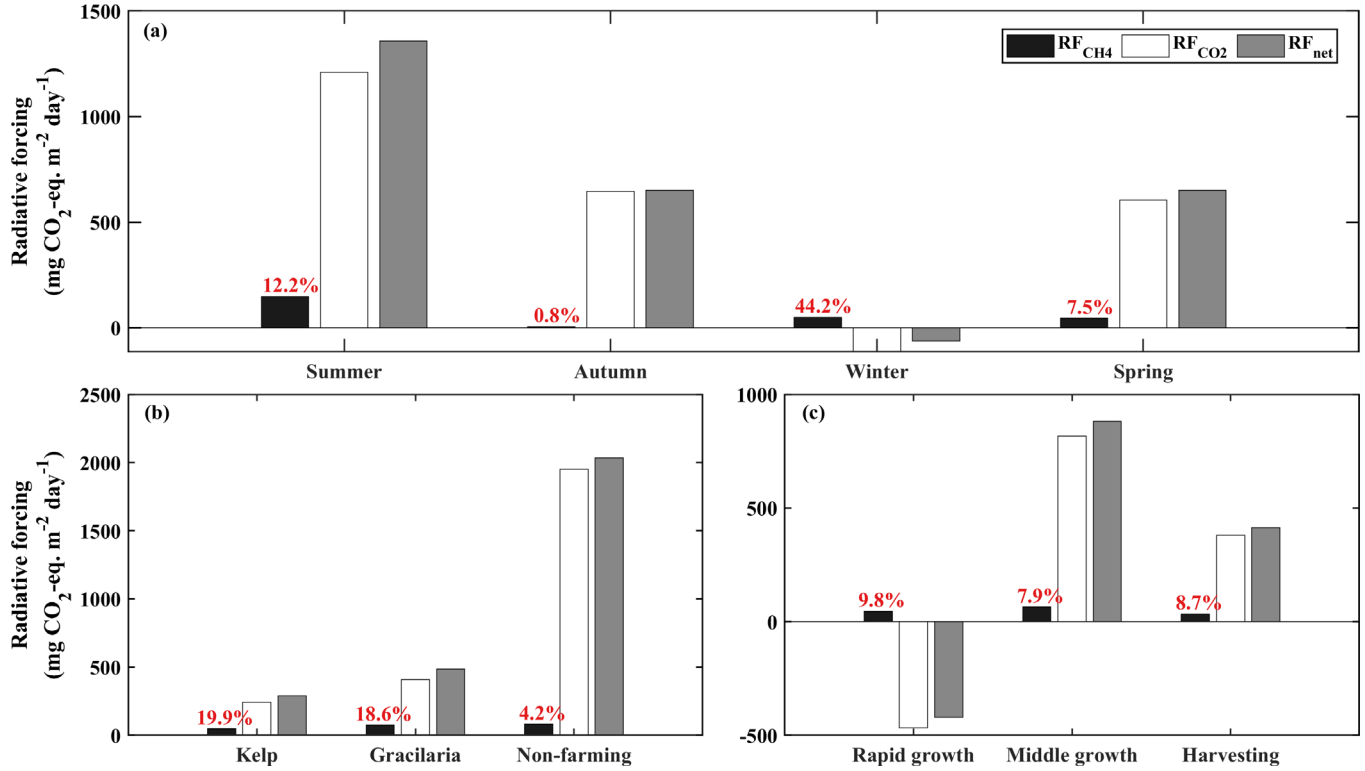

Fig. 8. Mean radiative forcing of net ecosystem exchanges of CH_4 (RF_{CH_4}) and CO_2 (RF_{CO_2}) as well as their net combination (RFnet) across various (**a**) seasons, (**b**) farming periods, and (**c**) growth stages of kelp farming. The radiative forcing values were quantified as CO_2 equivalent (CO_2-eq.) using the sustained-flux global warming potential metric for a 100-yr time horizon. The value above each RF_{CH_4} bar indicates the percentage of RF_{CH_4} over RF_{CO_2}.

magnitude across seasons, farming stages, and tidal levels (Figs. 7, 8). Despite being relatively low in the contribution of CH_4 emission on an annual scale, it should be taken into account in the assessments of radiative forcing in macroalgae aquaculture ecosystems. This is especially important during critical periods such as CO_2 depletion or low emission periods (Yang et al. 2018), when CH_4 emission may account for a large fraction of the total GHG budget.

Limitations and uncertainties

The field measurements and related data analyses of this study suffer from several limitations and uncertainties. First, the flux data unavoidably become biased as a result of flux corrections and quality control. For example, to reduce the uncertainty due to unbalanced day–night data availability, we have to first, respectively, perform quality control on daytime and nighttime data and then aggregate them into the daily and monthly data (X. Zhu, Ma, et al. 2024). Second, coastal ecosystems are susceptible to the terrestrial water inflows, which could favor a stronger source of CH_4 (Borges et al. 2018). However, given there is no river running into the aquaculture area where the EC tower is located, the confounding effects of background water inflows might be relatively small. Third, due to the high cost of the construction of the EC system in such a bay habitat experiencing severe weather (e.g., typhoons), we cannot afford to conduct paired EC measurements. Here we only analyzed and compared the impact of farming activities from the perspective of farming cycle without a control setup. Future research could use other approaches such as the floating chamber to improve the flux analysis regarding spatial heterogeneity. Finally, although the SGWP metric is used to evaluate the warming effect of CH_4 emission in this study, this metric only represents a specific effect over a fixed time period (Ma et al. 2024). Future application of dynamic SGWP metrics should improve the assessment of the radiative forcing of GHG fluxes at different time scales (Lynch et al. 2020).

Conclusions

One-year EC measurements of CH_4 fluxes over a subtropical macroalgae aquaculture ecosystem in southeast China were used in this study to examine the temporal variability of CH_4 fluxes across time scales and its contribution to the radiative forcing of CO_2 expressed as SGWPs. We confirm this ecosystem acts as a net CH_4 source on an annual scale with the flux fluctuations mainly driven by temperatures and tidal activities among seasons. Furthermore, for a 100-yr time horizon, annual CH_4 emission leads to a one-tenth increase in the warming effect from annual CO_2 emission. This is the first EC study to disentangle the temporal variability of NME and its

radiative contribution over macroalgae aquaculture ecosystems based on simultaneous measurements of both CH_4 and CO_2 fluxes. Although the ecosystem is confirmed as a biogeochemical hotspot of both CH_4 and CO_2 fluxes, their asynchronous flux variations complicate the assessments of their net radiative forcing. Future studies with multi-year EC measurements of continuous and high-frequency GHG fluxes are highly needed to further reduce the uncertainty in the assessments of GHG budgets and their radiative forcing in macroalgae aquaculture ecosystems.

Author Contributions

Yueting Deng: writing – original draft, visualization, investigation, data curation, formal analysis. Xianghui Guo: writing – review and editing, resources. Dengjin Hu: investigation. Hui Luo: visualization, investigation. Yougan Chen: writing – review and editing. Xudong Zhu: writing – review and editing, resources, supervision, project administration, funding acquisition, conceptualization.

Acknowledgments

This work was jointly supported by the Natural Science Foundation of Fujian Province of China (2023 J06008), the National Natural Science Foundation of China (32371661), the National Key Research and Development Program of China (2022YFF0802101, 2024YFF1306805), the Fujian Provincial Key Laboratory of Coast and Island Management Technology Study (FJCIMTS2024-02), the Shenzhen Science and Technology Plan Project (KCXST20221021111404011), and the 2023 Google Carbon Removal Research Awards.

Conflicts of Interest

None declared.

Data Availability Statement

Data will be made available on request.

References

Al-Haj, A. N., and R. W. Fulweiler. 2020. "A Synthesis of Methane Emissions From Shallow Vegetated Coastal Ecosystems." *Global Change Biology* 26, no. 5: 2988–3005. https://doi.org/10.1111/gcb.15046.

Arias-Ortiz, A., J. Wolfe, S. D. Bridgham, et al. 2024. "Methane Fluxes in Tidal Marshes of the Conterminous United States." *Global Change Biology* 30, no. 9: e17462. https://doi.org/10.1111/gcb.17462.

Attard, K. M., I. F. Rodil, P. Berg, J. Norkko, A. Norkko, and R. N. Glud. 2019. "Seasonal Metabolism and Carbon Export Potential of a Key Coastal Habitat: The Perennial Canopy-Forming Macroalga *Fucus vesiculosus*." *Limnology and Oceanography* 64, no. 1: 149–164. https://doi.org/10.1002/lno.11026.

Bach, L. T., V. Tamsitt, J. Gower, C. L. Hurd, J. A. Raven, and P. W. Boyd. 2021. "Testing the Climate Intervention Potential of Ocean Afforestation Using the Great Atlantic *Sargassum* Belt." *Nature Communications* 12, no. 1: 2556. https://doi.org/10.1038/s41467-021-22837-2.

Baldocchi, D. D. 2020. "How Eddy Covariance Flux Measurements Have Contributed to our Understanding of *Global Change Biology*." *Global Change Biology* 26, no. 1: 242–260. https://doi.org/10.1111/gcb.14807.

Borges, A. V., G. Speeckaert, W. Champenois, M. I. Scranton, and N. Gypens. 2018. "Productivity and Temperature as Drivers of Seasonal and Spatial Variations of Dissolved Methane in the Southern Bight of the North Sea." *Ecosystems* 21, no. 4: 583–599. https://doi.org/10.1007/s10021-017-0171-7.

Bridgham, S. D., H. Cadillo-Quiroz, J. K. Keller, and Q. Zhuang. 2013. "Methane Emissions From Wetlands: Biogeochemical, Microbial, and Modeling Perspectives From Local to Global Scales." *Global Change Biology* 19: 1325–1346. https://doi.org/10.1111/gcb.12131.

Dale, A. W., S. Flury, H. Fossing, et al. 2019. "Kinetics of Organic Carbon Mineralization and Methane Formation in Marine Sediments (Aarhus Bay, Denmark)." *Geochimica et Cosmochimica Acta* 252: 159–178. https://doi.org/10.1016/j.gca.2019.02.033.

Deng, Y., X. Guo, X. Zhao, et al. 2025. "Coastal Macroalgae Aquaculture Reduces Carbon Dioxide Emission in a Subtropical Enclosed Bay: Insights From Eddy Covariance Measurements." *Agriculture, Ecosystems & Environment* 385: 109576. https://doi.org/10.1016/j.agee.2025.109576.

Duarte, C. M., A. Bruhn, and D. Krause-Jensen. 2022. "A Seaweed Aquaculture Imperative to Meet Global Sustainability Targets." *Nature Sustainability* 5, no. 3: 185–193. https://doi.org/10.1038/s41893-021-00773-9.

Edson, J. B., A. A. Hinton, K. E. Prada, J. E. Hare, and C. W. Fairall. 1998. "Direct Covariance Flux Estimates From Mobile Platforms at Sea." *Journal of Atmospheric and Oceanic Technology* 15, no. 2: 547–562. https://doi.org/10.1175/1520-0426(1998)015<0547:DCFEFM>2.0.CO;2.

Ferrón, S., T. Ortega, and J. M. Forja. 2010. "Temporal and Spatial Variability of Methane in the North-Eastern Shelf of the Gulf of Cádiz (SW Iberian Peninsula)." *Journal of Sea Research* 64, no. 3: 213–223. https://doi.org/10.1016/j.seares.2010.02.007.

Gao, G., J. Beardall, P. Jin, L. Gao, S. Xie, and K. Gao. 2022. "A Review of Existing and Potential Blue Carbon Contributions to Climate Change Mitigation in the Anthropocene." *Journal of Applied Ecology* 59, no. 7: 1686–1699. https://doi.org/10.1111/1365-2664.14173.

Hall, N., W. W. Wong, R. Lappan, et al. 2025. "Coastal Methane Emissions Driven by Aerotolerant Methanogens Using Seaweed and Seagrass Metabolites." *Nature Geoscience* 18, no. 9: 854–861. https://doi.org/10.1038/s41561-025-01768-3.

Henriksson, L., Y. Y. Y. Yau, C. Majtényi-Hill, et al. 2024. "Drivers of Seasonal and Diel Methane Emissions From a Seagrass Ecosystem." *Journal of Geophysical Research: Biogeosciences* 129, no. 11: e2024JG008079. https://doi.org/10.1029/2024JG008079.

Hilt, S., H.-P. Grossart, D. McGinnis, and F. Keppler. 2022. "Potential Role of Submerged Macrophytes for Oxic Methane Production in Aquatic Ecosystems." *Limnology and Oceanography* 67, no. S2: S76–S88 . https://doi.org/10.1002/lno.12095.

Hou, J., G. Zhang, M. Sun, W. Ye, and D. Song. 2016. "Methane Distribution, Sources, and Sinks in an Aquaculture Bay (Sanggou Bay, China)." *Aquaculture Environment Interactions* 8: 481–495. https://doi.org/10.3354/aei00189.

Hurd, C. L., C. S. Law, L. T. Bach, et al. 2022. "Forensic Carbon Accounting: Assessing the Role of Seaweeds for Carbon Sequestration." *Journal of Phycology* 58, no. 3: 347–363. https://doi.org/10.1111/jpy.13249.

Jeffrey, L. C., D. T. Maher, S. G. Johnston, B. P. Kelaher, A. Steven, and D. R. Tait. 2019. "Wetland Methane Emissions Dominated by Plant-Mediated Fluxes: Contrasting Emissions Pathways and Seasons Within a Shallow Freshwater Subtropical Wetland." *Limnology and Oceanography* 64, no. 5: 1895–1912. https://doi.org/10.1002/lno.11158.

Jordan, S. F. A., T. Treude, I. Leifer, et al. 2020. "Bubble-Mediated Transport of Benthic Microorganisms Into the Water Column: Identification of Methanotrophs and Implication of Seepage Intensity on Transport Efficiency." *Scientific Reports* 10, no. 1: 4682. https://doi.org/10.1038/s41598-020-61446-9.

Knittel, K., and A. Boetius. 2009. "Anaerobic Oxidation of Methane: Progress With an Unknown Process." *Annual Review of Microbiology* 63, no. 1: 311–334. https://doi.org/10.1146/annurev.micro.61.080706.093130.

Kormann, R., and F. X. Meixner. 2001. "An Analytical Footprint Model for Non-Neutral Stratification." *Boundary-Layer Meteorology* 99: 207–224. https://doi.org/10.1023/A:1018991015119.

Krause-Jensen, D., and C. M. Duarte. 2016. "Substantial Role of Macroalgae in Marine Carbon Sequestration." *Nature Geoscience* 9, no. 10: 737–742. https://doi.org/10.1038/ngeo2790.

Li, J., J. Yuan, Y. Dong, et al. 2024. "Radiative Forcing of Methane Emission Completely Offsets Net Carbon Dioxide Uptake in a Temperate Freshwater Marsh From the Present to Future." *Agricultural and Forest Meteorology* 346: 109889. https://doi.org/10.1016/j.agrformet.2024.109889.

Liu, J., Y. Zhou, A. Valach, et al. 2020. "Methane Emissions Reduce the Radiative Cooling Effect of a Subtropical Estuarine Mangrove Wetland by Half." *Global Change Biology* 26, no. 9: 4998–5016. https://doi.org/10.1111/gcb.15247.

Liu, Y., and X. Zhu. 2024. "Tracking Mangrove Light Use Efficiency Using Normalized Difference Red Edge Index." *Ecological Indicators* 168: 112774. https://doi.org/10.1016/j.ecolind.2024.112774.

Lundevall-Zara, M., E. Lundevall-Zara, and V. Brüchert. 2021. "Sea–Air Exchange of Methane in Shallow Inshore Areas of the Baltic Sea." *Frontiers in Marine Science* 8: 657459. https://doi.org/10.3389/fmars.2021.657459.

Lynch, J., M. Cain, R. Pierrehumbert, and M. Allen. 2020. "Demonstrating GWP*: A Means of Reporting Warming-Equivalent Emissions That Captures the Contrasting Impacts of Short- and Long-Lived Climate Pollutants." *Environmental Research Letters* 15, no. 4: 044023. https://doi.org/10.1088/1748-9326/ab6d7e.

Ma, S., I. F. Creed, and P. Badiou. 2024. "New Perspectives on Temperate Inland Wetlands as Natural Climate Solutions Under Different CO_2-Equivalent Metrics." *Npj Climate and Atmospheric Science* 7, no. 1: 1–11. https://doi.org/10.1038/s41612-024-00778-z.

Mauder, M., M. Cuntz, C. Drüe, et al. 2013. "A Strategy for Quality and Uncertainty Assessment of Long-Term Eddy-Covariance Measurements." *Agricultural and Forest Meteorology* 169: 122–135. https://doi.org/10.1016/j.agrformet.2012.09.006.

McNicol, G., C. S. Sturtevant, S. H. Knox, I. Dronova, D. D. Baldocchi, and W. L. Silver. 2017. "Effects of Seasonality, Transport Pathway, and Spatial Structure on Greenhouse Gas Fluxes in a Restored Wetland." *Global Change Biology* 23, no. 7: 2768–2782. https://doi.org/10.1111/gcb.13580.

Neubauer, S. C., and J. P. Megonigal. 2015. "Moving Beyond Global Warming Potentials to Quantify the Climatic Role of Ecosystems." *Ecosystems* 18, no. 6: 1000–1013. https://doi.org/10.1007/s10021-015-9879-4.

Noyce, G. L., A. J. Smith, M. L. Kirwan, R. L. Rich, and J. P. Megonigal. 2023. "Oxygen Priming Induced by Elevated CO_2 Reduces Carbon Accumulation and Methane Emissions in Coastal Wetlands." *Nature Geoscience* 16, no. 1: 63–68. https://doi.org/10.1038/s41561-022-01070-6.

Ortega, A., N. R. Geraldi, I. Alam, et al. 2019. "Important Contribution of Macroalgae to Oceanic Carbon Sequestration." *Nature Geoscience* 12, no. 9: 748–754. https://doi.org/10.1038/s41561-019-0421-8.

Papale, D., M. Reichstein, M. Aubinet, et al. 2006. "Towards a Standardized Processing of Net Ecosystem Exchange Measured With Eddy Covariance Technique: Algorithms and Uncertainty Estimation." *Biogeosciences* 3: 571–583. https://doi.org/10.5194/bg-3-571-2006.

Pessarrodona, A., J. Howard, E. Pidgeon, T. Wernberg, and K. Filbee-Dexter. 2024. "Carbon Removal and Climate Change Mitigation by Seaweed Farming: A State of Knowledge Review." *Science of the Total Environment* 918: 170525. https://doi.org/10.1016/j.scitotenv.2024.170525.

Podgrajsek, E., E. Sahlée, D. Bastviken, et al. 2014. "Comparison of Floating Chamber and Eddy Covariance Measurements of Lake Greenhouse Gas Fluxes." *Biogeosciences* 11, no. 15: 4225–4233. https://doi.org/10.5194/bg-11-4225-2014.

Queirós, A. M., N. Stephens, S. Widdicombe, et al. 2019. "Connected Macroalgal-Sediment Systems: Blue Carbon and Food Webs in the Deep Coastal Ocean." *Ecological Monographs* 89, no. 3: e01366. https://doi.org/10.1002/ecm.1366.

Resplandy, L., A. Hogikyan, J. D. Müller, et al. 2024. "A Synthesis of Global Coastal Ocean Greenhouse Gas Fluxes." *Global Biogeochemical Cycles* 38, no. 1: e2023GB007803. https://doi.org/10.1029/2023GB007803.

Rosentreter, J. A., A. N. Al-Haj, R. W. Fulweiler, and P. Williamson. 2021. "Methane and Nitrous Oxide Emissions Complicate Coastal Blue Carbon Assessments." *Global Biogeochemical Cycles* 35, no. 2: e2020GB006858. https://doi.org/10.1029/2020GB006858.

Rosentreter, J. A., A. V. Borges, B. R. Deemer, et al. 2021. "Half of Global Methane Emissions Come From Highly Variable Aquatic Ecosystem Sources." *Nature Geoscience* 14, no. 4: 225–230. https://doi.org/10.1038/s41561-021-00715-2.

Rosentreter, J. A., D. T. Maher, D. V. Erler, R. H. Murray, and B. D. Eyre. 2018. "Methane Emissions Partially Offset 'Blue Carbon' Burial in Mangroves." *Science Advances* 4, no. 6: eaao4985. https://doi.org/10.1126/sciadv.aao4985.

Roth, F., E. Broman, X. Sun, et al. 2023. "Methane Emissions Offset Atmospheric Carbon Dioxide Uptake in Coastal Macroalgae, Mixed Vegetation and Sediment Ecosystems." *Nature Communications* 14, no. 1: 42. https://doi.org/10.1038/s41467-022-35673-9.

Roth, F., X. Sun, M. C. Geibel, et al. 2022. "High Spatiotemporal Variability of Methane Concentrations Challenges Estimates of Emissions across Vegetated Coastal Ecosystems." *Global Change Biology* 28, no. 14: 4308–4322. https://doi.org/10.1111/gcb.16177.

Schmale, O., I. Leifer, J. S. Deimling, et al. 2015. "Bubble Transport Mechanism: Indications for a Gas Bubble-Mediated Inoculation of Benthic Methanotrophs into the Water Column." *Continental Shelf Research* 103: 70–78. https://doi.org/10.1016/j.csr.2015.04.022.

Wallenius, A. J., P. Dalcin Martins, C. P. Slomp, and M. S. M. Jetten. 2021. "Anthropogenic and Environmental Constraints on the Microbial Methane Cycle in Coastal Sediments." *Frontiers in Microbiology* 12: 631621. https://doi.org/10.3389/fmicb.2021.631621.

Wang, X., and X. Zhu. 2024. "Salinity Stress and Atmospheric Dryness Co-Limit Evapotranspiration in a Subtropical Monsoonal Estuarine Mangrove Wetland." *Environmental Research Letters* 19, no. 11: 114067. https://doi.org/10.1088/1748-9326/ad8586.

Wang, Y., W. Yang, X. Zhao, et al. 2023. "Changes in the Carbon Source and Storage in a Cultivation Area of Macro-Algae in Southeast China." *Marine Pollution Bulletin* 188: 114680. https://doi.org/10.1016/j.marpolbul.2023.114680.

Wanninkhof, R., W. E. Asher, D. T. Ho, C. Sweeney, and W. R. McGillis. 2009. "Advances in Quantifying Air–Sea Gas Exchange and Environmental Forcing." *Annual Review of Marine Science* 1: 213–244. https://doi.org/10.1146/annurev.marine.010908.163742.

Wu, J., H. Zhang, Y. Pan, et al. 2020. "Opportunities for Blue Carbon Strategies in China." *Ocean and Coastal Management* 194: 105241. https://doi.org/10.1016/j.ocecoaman.2020.105241.

Xiong, T., H. Li, Y. Hu, et al. 2024. "Seaweed Farming Environments Do Not Always Function as CO_2 Sink Under Synergistic Influence of Macroalgae and Microorganisms." *Agriculture, Ecosystems & Environment* 361: 108824. https://doi.org/10.1016/j.agee.2023.108824.

Yang, P., Y. Zhang, D. Y. F. Lai, L. Tan, B. Jin, and C. Tong. 2018. "Fluxes of Carbon Dioxide and Methane Across the Water–Atmosphere Interface of Aquaculture Shrimp Ponds in Two Subtropical Estuaries: The Effect of Temperature, Substrate, Salinity and Nitrate." *Science of the Total Environment* 635: 1025–1035. https://doi.org/10.1016/j.scitotenv.2018.04.102.

Yau, Y. Y. Y., G. Reithmaier, C. Majtényi-Hill, et al. 2023. "Methane Emissions in Seagrass Meadows as a Small Offset to Carbon Sequestration." *Journal of Geophysical Research: Biogeosciences* 128, no. 6: e2022JG007295. https://doi.org/10.1029/2022JG007295.

Yvon-Durocher, G., A. P. Allen, D. Bastviken, et al. 2014. "Methane Fluxes Show Consistent Temperature Dependence Across Microbial to Ecosystem Scales." *Nature* 507, no. 7493: 488–491. https://doi.org/10.1038/nature13164.

Zhang, Y. F., K. Tang, P. Yang, et al. 2022. "Assessing Carbon Greenhouse Gas Emissions From Aquaculture in China Based on Aquaculture System Types, Species, Environmental Conditions and Management Practices." *Agriculture, Ecosystems & Environment* 338: 108110. https://doi.org/10.1016/j.agee.2022.108110.

Zhang, Y. P., Z. Qin, T. Li, and X. Zhu. 2022. "Carbon Dioxide Uptake Overrides Methane Emission at the Air–Water Interface of Algae-Shellfish Mariculture Ponds: Evidence From Eddy Covariance Observations." *Science of the Total Environment* 815: 152867. https://doi.org/10.1016/j.scitotenv.2021.152867.

Zhang, Y., X. Guo, and X. Zhu. 2023. "Strong Diurnal Variability of Carbon Dioxide Flux over Algae-Shellfish Aquaculture Ponds Revealed by Eddy Covariance Measurements." *Agriculture, Ecosystems & Environment* 348: 108426. https://doi.org/10.1016/j.agee.2023.108426.

Zhu, X., C. Sun, and Z. Qin. 2021. "Drought-Induced Salinity Enhancement Weakens Mangrove Greenhouse Gas Cycling." *Journal of Geophysical Research: Biogeosciences* 126, no. 8: e2021JG006416. https://doi.org/10.1029/2021JG006416.

Zhu, X., J. Chen, L. Li, et al. 2024. "Asynchronous Methane and Carbon Dioxide Fluxes Drive Temporal Variability of Mangrove Blue Carbon Sequestration." *Geophysical Research Letters* 51, no. 11: e2023GL107235. https://doi.org/10.1029/2023GL107235.

Zhu, X., L. Song, Q. Weng, and G. Huang. 2019. "Linking In Situ Photochemical Reflectance Index Measurements with Mangrove Carbon Dynamics in a Subtropical Coastal Wetland." *Journal of Geophysical Research: Biogeosciences* 124, no. 6: 1714–1730. https://doi.org/10.1029/2019JG005022.

Zhu, X., M. Ma, L. Li, and M. Li. 2024. "Impacts of Intensive Smooth Cordgrass Removal on Net Ecosystem Exchange in

a Saltmarsh-Mangrove Ecotone of Southeast China." *Science of the Total Environment* 934: 173202. https://doi.org/10.1016/j.scitotenv.2024.173202.

Zhu, X., Y. Hou, Y. Zhang, X. Lu, Z. Liu, and Q. Weng. 2021. "Potential of Sun-Induced Chlorophyll Fluorescence for Indicating Mangrove Canopy Photosynthesis." *Journal of Geophysical Research: Biogeosciences* 126, no. 4: e2020JG006159. https://doi.org/10.1029/2020JG006159.

Zhu, X., Z. Qin, and L. Song. 2021. "How Land-Sea Interaction of Tidal and Sea Breeze Activity Affect Mangrove Net Ecosystem Exchange?" *Journal of Geophysical Research: Atmospheres* 126, no. 8: e2020JD034047. https://doi.org/10.1029/2020JD034047.

Zhu, X., Z. Qin, W. Liu, et al. 2025. "Coastal Restoration May Not Necessarily Enhance Blue Carbon Sink." *Geophysical Research Letters* 52: e2025GL114614. https://doi.org/10.1029/2025GL114614.

Zhu, Z., and X. Zhu. 2025. "Increasing Midday Depression of Mangrove Photosynthesis With Heat and Drought Stresses." *Agricultural and Forest Meteorology* 362: 110372. https://doi.org/10.1016/j.agrformet.2024.110372.

Supporting Information

Additional Supporting Information may be found in the online version of this article.

Submitted 06 March 2025
Revised 16 October 2025
Accepted 04 December 2025